

Mathematical model of the spinning of microstructured fibres

Christopher J. Voyce and Alistair D. Fitt

*School of Mathematics, University of Southampton,
Southampton SO17 1BJ, U.K.*

cjv@maths.soton.ac.uk

Tanya M. Monro

*Optoelectronics Research Centre, University of Southampton,
Southampton SO17 1BJ, U.K.*

Abstract: We construct a fluid mechanics model of the drawing of microstructured optical fibres ('holey fibres'). This model can be used to understand and quantify methods for controlling the fibre geometry. The effects of preform rotation are included to examine methods for reducing fibre birefringence. Asymptotic numerical-solutions are obtained and applied to two typical microstructured-fibres and a number of practical suggestions are made for achieving sub-mm spin pitches without damaging the microstructure within.

© 2004 Optical Society of America

OCIS codes: (220.0220) Optical design and fabrication.

References and links

1. R.S. Ranka, A.J. Stentz, "Optical properties of high-delta air-silica microstructure optical fibers," *Opt. Lett.* **25**, 796–798 (2000).
2. T.M. Monro, D.J. Richardson, N.G.R. Broderick, P.J. Bennett, "Holey optical fibers: An efficient modal model," *J. Lightwave Technol.* **17**, 1093–1102 (1999).
3. T.M. Monro, D.J. Richardson, P.J. Bennett, "Developing holey fibres for evanescent field devices," *Elect. Lett.* **35**, 1188–1189 (1999).
4. A.J. Barlow, J.J. Ramskov-Hansen, D.N. Payne, "Birefringence and polarization mode dispersion in spun single-mode fibres," *Applied Optics* **30**, 2962–68 (1981).
5. M.J. Li, D.A. Nolan, "Fiber spin-profile designs for producing fibers with low polarization mode dispersion," *Opt. Lett.*, **23**, 1659–1661 (1998).
6. R.E. Schuh, X. Shan, A. Shamim Siddiqui, "Polarization Mode Dispersion in Spun Fibers with Different Linear Birefringence and Spinning Parameters," *J. Lightwave Technol.* **16**, 1583–1588 (1998).
7. M. Fuchii, J.R. Hayes, K. Furusawa, W. Belardi, J.C. Baggett, T. M. Monro, D.J. Richardson, "Polarization mode dispersion reduction in spun large mode area silica holey fibres," *Opt. Express* **9**, 1972–1977 (2004), <http://www.opticsexpress.org/abstract.cfm?URI=OPEX-12-9-1972>.
8. J.P. Gordon, H. Kogelnik, "PMD Fundamentals: Polarization mode dispersion in optical fibers," *PNAS* **97** (9), 4541–4550 (2000).
9. A. Ortigosa-Blanch, J.C. Knight, W.J. Wadsworth, J. Arriaga, B.J. Mangan, T.A. Birks, St. J. Russell, "Highly birefringent photonic crystal fibers," *Opt. Lett.* **25**, 1325–1327 (2000).
10. J.R. Hayes, Optoelectronics Research Centre, University of Southampton, University Road, Southampton, Hampshire, SO17 1BJ, U.K. (personal communication, 2003).
11. A.D. Fitt, K. Furusawa, T.M. Monro, C.P. Please, "Modelling the fabrication of hollow fibers: capillary drawing," *J. Lightwave Technol.* **31**, 1924–31 (2001).
12. A.D. Fitt, K. Furusawa, T.M. Monro, C.P. Please, D.J. Richardson, "The mathematical modelling of capillary drawing for holey fibre manufacture," *J. Eng. Math.* **43**, 201–227 (2002).
13. C.J. Voyce, School of Mathematics, University of Southampton, Southampton, SO17 1BJ, U.K., A.D. Fitt and T.M. Monro are preparing a manuscript to be called "The mathematical modelling of spun capillaries."

14. R.H. Doremus, "Viscosity of silica," *J. Appl. Phys.* **92**, 7619-7629 (2002).
 15. T.M. Monro, K. Furusawa, J.H. Lee, J.H.V. Price, Z. Yusoff, J.C. Baggett, D.J. Richardson, "Advances in holey fibers," in *Advances in Fiber Lasers*, L.N. Durvasula, ed., Proc. SPIE **4974**, 83-95 (2003).
 16. P.K.A. Wai, W.L. Kath, C.R. Menyuk, J.W. Zhang, "Nonlinear polarization-mode dispersion in optical fibers with randomly varying birefringence," *J. Opt. Soc. Am. B* **14**, 2967-2979 (1997).
 17. U.C. Paek, "Free Drawing and Polymer Coating of Silica Glass Optical Fibers," *ASME Journal of Heat Transfer* **121**, 774-789 (1999).
 18. P. Petropoulos, H. Ebendorff-Heidepriem, V. Finazzi, R.C. Moore, K. Frampton, D.J. Richardson, T.M. Monro, "Highly nonlinear and anomalously dispersive lead silicate glass holey fibers," *Opt. Express* **11**, 3568-3573 (2003), <http://www.opticsexpress.org/abstract.cfm?URI=OPEX-11-26-3568>.
 19. C.J. Joyce, A.D. Fitt, T.M. Monro, "Mathematical modelling of the drawing of spun capillary tubes," in *Progress in Industrial Mathematics at ECMI 2002*, A. Buikis, R. Ciegis, A.D. Fitt, eds. (Springer-Verlag, Berlin, 2004), pp. 387-391.
-

1. Introduction

Microstructured optical-fibres contain a lattice of air holes surrounding a solid core. The presence of air holes lowers the effective refractive-index, and the effective refractive-index difference allows the fibre to guide light [1, 2, 3]. Although at first sight this guidance mechanism is similar to that operating in a conventional optical fibre, microstructured fibres exhibit a host of highly unusual and tailorable optical properties.

Microstructured optical fibres are manufactured by heating a macroscopic structured-preform (typically a few centimetres in diameter), and drawing it down to the required dimensions (typically $125\mu\text{m}$). The presence of air holes in the cross-section presents both challenges and opportunities for the fabrication of these fibres. Competition between viscosity and surface-tension effects can alter the size and shape of the holes during the drawing process, and in extreme cases hole closure can occur. Since the fabrication of structured preforms is one of the most labour intensive parts of the manufacturing process, it is often desirable to produce a number of different fibre profiles from a single preform by changing the conditions under which the fibre is drawn.

Conventional (solid) preforms are routinely rotated to introduce a twist into the final fibre, since this reduces polarization mode dispersion (PMD) [4, 5, 6]. It is not obvious that the same process may be applied to holey-fibre preforms without producing adverse macroscopic geometry-changes that severely compromise the microstructure within. Preservation of the microstructure has recently been demonstrated when rotating large mode-area fibres with a high density of small, dispersed holes, at rates sufficient to dramatically improve PMD [7].

Fibre birefringence provides another reason for spinning during the fibre manufacture process. Its effects can be significant in holey fibres for three main reasons [8]. Firstly, many of these fibres have wavelength-scale structures. Secondly, a significant refractive index contrast may exist between the core and the effective refractive-index of the cladding. Thirdly, intended or accidental geometrical asymmetries may be introduced in the manufacturing process, which may include the locking in of some asymmetric stress-distribution within the fibre [9]. When such asymmetries are present in holey fibres, exacerbated by the high refractive-index contrast, the two polarizations of light travel at different speeds. This results in fibre birefringence with a characteristic beat-length, caused by the components of light interfering as they travel at different rates, which may be as short as 0.3mm (see section 3).

In sensor applications where maintaining polarization is desirable to improve isolation between the modes by maximizing the mode splitting, fibre birefringence is desirable. In data transmission and other applications fibre birefringence is unwanted and can be reduced by averaging out the effects of asymmetries along the fibre by introducing a twist [4]. The periodicity of the twist required depends on the wavelength of light and the details of the fibre profile. Fibre preforms can be rotated as they enter the furnace and held with zero rotation at its exit, leaving

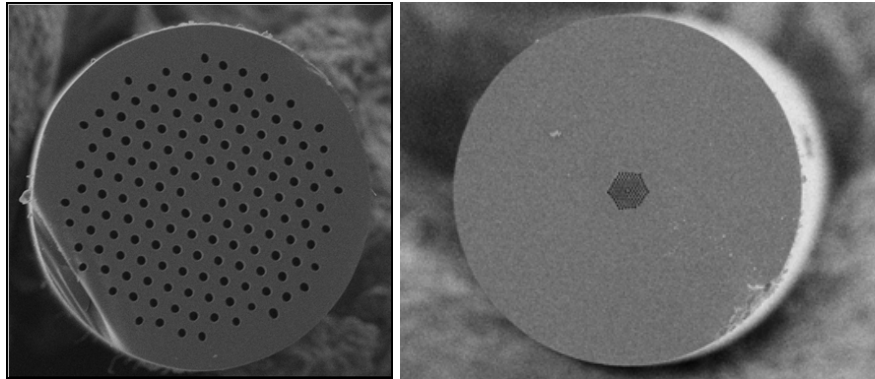


Fig. 1. (Left) The cross-section of a type-one holey fibre. (Right) The cross-section of a type-two holey fibre.

the fibre with an overall twist along its length [7]. This stratagem succeeds provided the twist periodicity (spin pitch) does not exceed the beat length. However, there is currently a practical limit of about 2000rpm to the rate at which preforms may be rotated. At rates greater than this, the alignment of the preform in the furnace becomes unstable and the preform begins to vibrate [10].

Evidently holey-fibre technology would be greatly aided by the development of accurate tools for predicting the changes that occur during fibre drawing. We have developed a mathematical model to examine the effects of preform rotation on microstructured-fibre drawing. Our model considers a single capillary tube, which is a realistic approximation for the two specific fibre-types described below. We regard this as a first-step towards modelling the general microstructured-fibre fabrication problem. Below, we use this model to answer three questions: (i) can we reduce or remove fibre birefringence at realistic rotation rates whilst preserving the microstructure? (ii) can we minimize the spin pitch in fibres by other means whilst remaining within the rotation limit and preserving the microstructure? (iii) can we use preform spinning as a method for controlling the fibre geometry?

The first type of fibre considered is a large mode-area holey fibre with an approximately uniform distribution of diffuse holes. This will be referred to as a “type-one” holey fibre (see Fig. 1), and might be useful for transmission, where there is a need to reduce PMD. These are manufactured in a single stage, the preform being assembled and then drawn directly into fibre form. Secondly, we consider fibres where a large jacket surrounds a microstructured region with a high density of holes. These fibres have small core-dimensions and outer dimensions that allow the fibre to be handled easily. These will be referred to as “type-two” holey fibres (see Fig. 1), and are useful for non-linear devices in which the reduction of birefringence is often a critical issue. Type-two fibres are typically manufactured in two stages. A “cane” preform (comprising the microstructured region in the final fibre) is drawn to a cane. The cane is then inserted into a “jacket tube” (capillary tube) and the resulting structure drawn to produce a fibre. In principle these fibres could be manufactured in a single-stage process with a suitable drawing furnace.

We assume throughout that the glass used is Suprasil F300, a silica glass commonly used in the production of high-quality silica optical-fibres. The physical properties used for the computations were taken from [11].

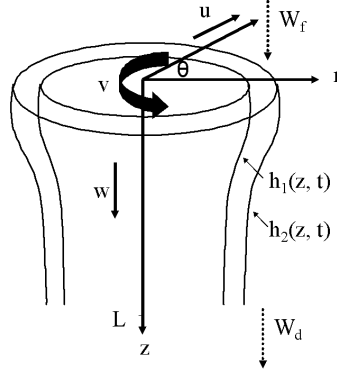


Fig. 2. Problem geometry and nomenclature.

2. Mathematical modelling

To develop a model for capillary drawing that is capable of including the effects of internal hole–pressurization, viscosity, surface tension, gravity and rotation, we begin with the Navier–Stokes Eqs. in cylindrical coordinates, and use a methodology related to that set out in [12]. A schematic diagram of the capillary geometry is shown in Fig. 2. The inner and outer capillary–radii are denoted by h_1 and h_2 . W_f and W_d are velocity boundary–conditions at the top and bottom of the furnace respectively.

We assume that the flow is axisymmetric, and therefore independent of the azimuthal angle θ . The velocity \mathbf{q} of the molten glass is denoted by $\mathbf{q} = w\mathbf{e}_z + u\mathbf{e}_r + v\mathbf{e}_\theta$, where \mathbf{e}_z , \mathbf{e}_r and \mathbf{e}_θ are unit vectors in the z , r and θ directions respectively; $v \neq 0$ when rotation is present.

Space permits only the briefest details of the model derivation [13]. After appropriate non-dimensionalizations, an asymptotic analysis of the governing Eqs., based on the small aspect ratio (radius/length) of the preform, eventually leads to the (dimensional) isothermal Eqs.

$$\rho(h_2^2 - h_1^2)(w_{0t} + w_0 w_{0z} - g) = [3\mu(h_2^2 - h_1^2)w_{0z} + \gamma(h_1 + h_2) + \frac{\rho}{4}(h_2^4 - h_1^4)B^2]_z, \quad (1)$$

$$(h_1^2)_t + (h_1^2 w_0)_z = \frac{2p_0 h_1^2 h_2^2 - 2\gamma h_1 h_2 (h_1 + h_2) + \rho h_1^2 h_2^2 B^2 (h_2^2 - h_1^2)}{2\mu(h_2^2 - h_1^2)}, \quad (2)$$

$$(h_2^2)_t + (h_2^2 w_0)_z = \frac{2p_0 h_1^2 h_2^2 - 2\gamma h_1 h_2 (h_1 + h_2) + \rho h_1^2 h_2^2 B^2 (h_2^2 - h_1^2)}{2\mu(h_2^2 - h_1^2)}, \quad (3)$$

$$\begin{aligned} \mu((h_2^4 - h_1^4)B_z)_z &= \rho[h_2^2(h_2^2 B)_t - h_1^2(h_1^2 B)_t] + \rho w_0[h_2^2(h_2^2 B)_z - h_1^2(h_1^2 B)_z] \\ &\quad - \frac{\rho\gamma B}{\mu}(h_1^2 h_2 + h_2^2 h_1) + \frac{\rho^2 B^3}{2\mu}(h_1^2 h_2^4 - h_2^2 h_1^4) + \frac{\rho}{\mu} p_0 B h_1^2 h_2^2, \end{aligned} \quad (4)$$

where the boundary conditions for the flow are given by

$$w(0, t) = W_f, \quad w(L, t) = W_d, \quad h_1(0, t) = h_{10}, \quad h_2(0, t) = h_{20}, \quad B(0, t) = B_0, \quad B(L, t) = B_L.$$

Here, density, dynamic viscosity, acceleration due to gravity, surface tension and hole over–pressure (i.e. the excess over atmospheric) are denoted by ρ , μ , g , γ and p_0 respectively. w_0 denotes the leading order term in w , and B denotes the variable v_0/r , which may be thought of as an angular frequency. Subscripts t and z denote differentiation with respect to time and

distance along the axis of the capillary respectively. When the preform rotation is zero, the Eqs. reduce to those derived in [12].

Consistent with [12], the surface tension of silica is taken to be $\gamma=0.3\text{N/m}$ and a draw length of $L = 3\text{cm}$ is assumed throughout. Since an efficient furnace gives an approximately-constant temperature throughout we ignore the effects of heat transfer in assuming that the temperature of the glass is uniform. The viscosity law used for pure silica glass was taken from [14] and is given by

$$1400\text{C} \leq T \leq 2500\text{C} \quad \mu = 5.8 \times 10^{-7} \exp(515400/(8.3145T + 2271.10567)) \quad (\text{Poise}).$$

Numerical solutions of Eqs. (1)–(4) will be used later to quantify the effects of rotation on capillary geometry. First we shall define and examine the key properties of “spin pitch” for optical fibres.

2.1. Spin pitch in microstructured fibres

For a typical fibre angular-frequency Ω/ε , where $\varepsilon = h/L \ll 1$ is the ratio of a typical preform radius h to L , the preform rotation rate is easily quantified using the non-dimensional parameter $S = \frac{\Omega L}{W}$. The Reynolds number, which characterizes the relative importances of viscosity and inertia, is given by $Re = \frac{LW\rho}{\mu_0}$, where W and μ_0 are a typical downstream fluid velocity and viscosity respectively. In the physically realistic case with a rotation rate of approximately 1000rpm and a typical preform geometry, S^2 is $O(1)$ and $Re \ll 1$. It is then appropriate to ask how we might determine the spin pitch, since one might expect it to depend on the functional form of the solutions to the governing Eqs. and therefore be non-trivial.

To do this we consider a steady-state process and define the angle ϕ to be the number of radians through which a fluid element has rotated as it traverses the z -axis from the furnace inlet to exit. ϕ changes with the time t' that a given point in the fibre has been in the furnace. If we know the rate at which ϕ changes with time at the end of the furnace, we can directly calculate the spin pitch d at a point z using

$$d(z) = \frac{2\pi w_0(z)}{\frac{\partial \phi}{\partial t'}}. \quad (5)$$

To derive an Eq. for $\phi(z, t')$ we follow a fluid element as the fibre is drawn to obtain

$$\phi_{t'} + w_0(z)\phi_z = B(z), \quad (6)$$

with

$$\phi(0, t') = B(0)t'.$$

This has the general solution

$$\phi(z, t') = B(0)t' + \int_0^z \frac{[B(z') - B(0)] dz'}{w_0(z')}.$$

Substituting this into Eq. (5) and evaluating at the point $z = L$ yields the final spin-pitch

$$d(L) = \frac{2\pi W_d}{\frac{\partial \phi}{\partial t'}|_{z=L}} = \frac{2\pi W_d}{B(0)}. \quad (7)$$

This can be interpreted as showing that, in the physically realistic limits assumed, the fibre rotates as though it were a solid body with the usual $v = r\omega$ form for the azimuthal fluid velocity, where ω is the angular frequency of rotation.

3. The effect of preform rotation on solid fibres

Though the practice of spinning solid optical fibres to reduce fibre birefringence is well established [4], the spinning of microstructured fibres has only recently been reported in [7], where a significant reduction in PMD was achieved. It would therefore be valuable to know whether it is possible to spin microstructured fibres at a rate necessary to remove fibre birefringence whilst preserving the microstructure. Beat lengths as small as 0.3mm have been measured [9, 15] in fibres with wavelength-scale features and a large refractive-index contrast. Currently, the smallest spin-pitch measured in a spun holey-fibre appears to be 1.23cm [7] and a sub-mm spin pitch is desirable.

We first examine the effect of rotation rate on the geometry of a solid fibre ($h_1 = 0$). When Eqs. (1)–(4) are presented in non-dimensional form, it is clear that Eq. (4) decouples from Eq. (1) when the rotation is less than a certain value. For steady-state fibre drawing, ignoring the complications of inertial forces, surface tension, hole pressurisation and gravity, we find that

$$3\bar{\mu}(\bar{h}_2^2\bar{w}_{0z})_z \cong -\frac{1}{4}ReS^2(\bar{h}_2^4\bar{B}^2)_z, \quad (8)$$

where overbars denote non-dimensional quantities whose scalings can be found in [13]. Substituting for the non-dimensional parameters shows that rotation therefore first begins to influence fibre geometry when

$$\frac{\Omega}{\varepsilon} \cong \frac{2}{h} \sqrt{\frac{3\bar{\mu}\mu_0 W}{L\rho}}. \quad (9)$$

Various realistic drawing-parameters could be chosen and substituted into Eq. (9) to determine the rotation rate at which geometry is affected. If we assign a glass viscosity and other parameters that give rise to the earliest onset of geometry change, Eq. (9) shows that this occurs when $\frac{\Omega}{\varepsilon} \approx 2900$ rpm. Full numerical-solutions of Eqs. (1)–(4), including the factors neglected in deriving Eq. (9) corroborate this. Whilst it is possible to rotate preforms at such a rate [16], vibrations and instabilities are often encountered in practice. Additionally, these drawing parameters were chosen specifically to create geometry change at low rotation rates, and in everyday draw scenarios much larger rotation rates will be possible with no effect on fibre geometry. We thus conclude that preform rotation will not generally affect the geometry of solid fibres. Although the point at which geometry of a microstructured fibre is modified may be somewhat different, Eq. (9) provides a useful first approximation in certain limiting cases that will be examined below.

3.1. Numerical results for capillary tubes

A great many asymptotic limits of the Eqs. (1)–(4) may be considered. These can show whether it is possible to prevent surface-tension induced hole-collapse by rotating the preform, whether preform rotation may act as a useful control of hole size, and be used to investigate other possible control mechanisms. We do not examine these limits here, referring the reader to [13]. Instead, we consider briefly the results of numerical studies of the steady version of the Eqs. using standard numerical library-routines to solve the boundary value problem.

Figure 3 shows numerical results for rotation of both a thin- and a thick-walled capillary. The general effect of rotating the preform as it enters the furnace is to increase both the inner and outer radii of the fibre along the entirety of the draw length. Preform rotation may thus be used as an additional control in the drawing process, since it is the fibre dimensions at the end of the furnace that primarily concern us. We also note that rotation appears to act on the fibre in a way that counteracts the effects of surface tension, which otherwise tends to close the air holes in the fibre. As well as reducing birefringence, rotation may thus, for example, allow

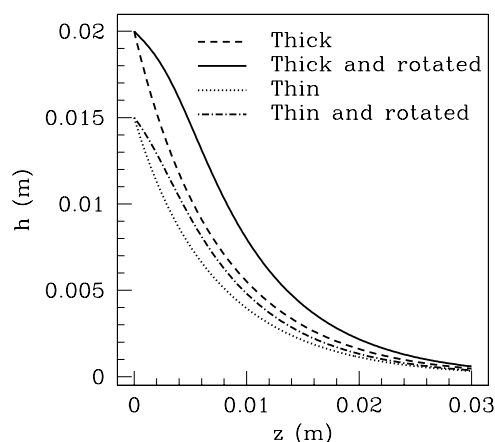


Fig. 3. The effects of preform rotation on outer capillary radius. The diagram shows the outer radius h_2 for fibre pulls with and without rotation. The thin-walled tube has $h_1(0) = 0.01\text{m}$, $h_2(0) = 0.015\text{m}$ and the thick-walled tube has $h_1(0) = 0.01\text{m}$, $h_2(0) = 0.02\text{m}$. (Draw length $L = 0.03\text{m}$, temperature $T = 2200\text{C}$, draw speed $W_d = 25\text{m/min}$, feed speed $W_f = 15\text{mm/min}$, rotation rate $\Omega = 35\text{rad/s}$.)

fibres to be drawn at increased temperatures or reduced tensions. This may be advantageous from a manufacturing viewpoint, as fibres drawn at high temperatures often possess superior strength [17].

It is also clear from Fig. 3 that the thick-walled capillary experiences a much greater deformation than the thin-walled. This is largely because the initial outer radius of the thick-walled capillary is larger than that of the thin-walled capillary. Comparison of the changes in fibre radii reveals that for both thin- and thick-walled tubes, the inner radius increases more than the outer. This occurs because the outer wall of the preform reacts to the effects of preform rotation (as a result of the ‘centrifugal force’). The inner wall is then modified in accordance with mass conservation conditions, which require it to be modified more heavily and thus increase the OD/ID ratio. The implications of this analysis will be discussed in the following section.

3.2. The effects of preform rotation on microstructured fibres

We have already shown that the spin pitch is determined uniquely by the draw speed and the rotation rate of the preform. The spin pitch calculation is valid for solid fibres, capillary tubes and microstructured fibres, since nothing in the derivation required the preform to be solid.

We now discuss the impact of preform rotation on the two specific fibre-types detailed in the introduction.

3.2.1. Type-one holey fibres

In the limit that the holes in the microstructured fibre are sparse (large mode-area fibres), we may safely assume that the effects of rotation on the geometry of these type-one microstructured fibres are approximately the same as in the solid-fibre case.

Microstructured fibres are generally pulled at a draw speed between 3 and 30m/min, depending upon the final geometry of the fibre and the structure of the preform. If fibre birefringence

is to be significantly reduced or removed, the twists must be on a scale equal to or less than that of the beat length, which is typically between 1 and 20mm.

It is tempting to consider the practically-desirable case of the maximum draw speed and the minimum spin-pitch, in order to discover the rate of preform rotation required. We can then consider whether this rotation rate will affect the geometry. However the rate of rotation is usually limited to about 2000rpm and overcoming this rotation rate limit by reducing the drawing speed would provide the desired spin-pitch, but will not produce the required fibre geometry unless the dimensions of the initial preform are accordingly reduced. Equation (7) shows that for a moderately low draw speed of 1m/min, the rotation rate needed to produce a spin pitch of between 1 and 20mm is between 1000rpm and 50rpm respectively. Assuming a typical silica glass viscosity of 2×10^5 poise, a draw length of 3cm and an initial preform diameter of 2cm, Eq. (9) predicts that the resulting geometry of type-one fibres will not be significantly modified at such rotation rates.

Addressing the questions posed in the introduction, it is clear that starting with a standard preform and pulling at typical draw speeds, practical limits will prevent the preform from being rotated rapidly enough to significantly reduce fibre birefringence. However, a 1mm spin pitch may be obtained by breaking the manufacture into two stages and drawing the final fibre more slowly. The first stage would be used to obtain a preform for the second stage of production, whose size is small enough to allow the production of a small diameter fibre despite the low draw-speed. Finally, our assumption that type-one fibres behave as solid fibres does not allow us to address the question of geometry control since solid fibres have a geometry uniquely determined by the velocity boundary-conditions and the preform dimensions.

3.2.2. Type-two holey fibres

When the microstructured portion of a holey fibre preform is surrounded by a thick jacket-tube and the density of holes in the microstructured region is large, we may approximate the holey fibre preform by a capillary tube. The large air-fraction holey cladding may be represented by the air hole in the centre of the capillary tube and the jacket by the glass region of a capillary tube cross-section. This is tantamount to assuming that the large air-fraction holey cladding has no significant impact on the behaviour of the solid jacket when spun. We can thus determine how the geometry of the fibre varies when spun by treating the whole structure as a capillary tube. The manner in which it is modified will then give an insight into whether the microstructured region will remain intact.

As mentioned previously, it is desirable to obtain a spin pitch in the holey fibre of about 1mm. Equation (7) shows that this may be accomplished either by applying a large rotation-rate or a small draw-speed.

Numerical calculations using Eqs. (1)–(4) show that capillary tubes whose initial outer diameter (OD) is as small as 1cm suffer significant geometry changes to both the inner- and outer-radii as a result of rotating the capillary tubes at 2000rpm and above. Capillary tubes with larger initial dimensions suffer even more of an effect. This distortion at lower rotation results from the presence of the hole in the capillary-tube preform, representing the microstructure. When a one-step drawing process is employed, the initial dimensions of the preforms are too large to prevent rotation affecting the geometry of the final fibre. This is crucial because such changes will modify the microstructure of the fibre. If the geometry of the microstructure (modelled as the hole in the capillary) changes too rapidly at the top of the furnace, the fluid will not have time to react to this change and the structure within will surely be destroyed. However, if such changes take place gradually over the length of the draw it is reasonable to assume that the microstructure will be modified but will remain intact.

Further numerical studies of Eqs. (1)–(4) show that when a preform is rotated the inner

diameter (ID) is increased, compared to the unrotated case, at every point along the furnace. The bulk of this increase occurs at the top of the furnace and in some cases (where a large furnace temperature is simulated, for example) the ID actually increases at the top of the furnace before being decreased by the draw-down process lower in the furnace. This suggests that as the preform enters the furnace it immediately expands as a result of the 'centrifugal force'. This initial expansion will surely have significant consequences for the survival of the microstructure as discussed above. It is less clear what might happen to the microstructure when the rotation steadily modifies the capillary geometry as it moves through the furnace, resulting in a final geometry slightly different from that produced without rotation. However, it may be assumed that the microstructure survives but its internal properties will be modified. We must therefore search for conditions under which type-two fibres may be drawn with a 1mm spin pitch whilst also attempting to minimize the effect of preform rotation on the fibre geometry, particularly towards the top of the furnace.

The practical implication of this is that the rotation rate must be kept as low as possible, requiring us to draw the fibre slowly to achieve a small spin-pitch. Unfortunately, it is hard to manufacture fibres with a highly consistent geometry along the length of the fibre when the draw speed is extremely low. If we assume a minimum draw speed of 1m/min, a preform rotation rate of 1000rpm is required to achieve a spin pitch of 1mm.

We now examine in detail how we may rotate a type-two preform to achieve a 1mm spin pitch. Equations (1)–(4) were solved numerically for a variety of drawing scenarios aimed at minimizing the final geometry change. Some examples are now given for a final fibre whose holey fibre cladding is 15–30 μm in diameter and whose jacket has diameter 80–300 μm . The core dimensions are chosen to be large enough to confine light well but small enough not to be difficult to produce or to weaken the fibre. The jacket dimensions are chosen to make the fibre sufficiently robust.

When the manufacture of these fibres is completed in a single stage, the initial diameter of the preform must be large (typically a few centimetres). A minimum size for the holey cladding in the preform exists because of practical difficulties in stacking canes with $\text{OD} \ll 1\text{mm}$, which in turn sets a minimum diameter for the jacket. If the preform is rotated during drawing, the initial jacket diameter and drawing rate must both be increased to obtain the same fibre geometry as would be produced without rotation. This results from the effects of rotation on the OD/ID ratio, described in section 3.1.

Let us consider a preform with a jacket diameter of 15mm and a holey-cladding diameter of 10mm. Whilst these particular diameters would never be chosen to make a fibre, they clearly show the possible effects of rotation on the microstructure. To obtain the fibre-geometry required, the feed speed is set to 1mm/min, the draw speed to 40m/min and temperature to 2000C. With no rotation a final holey-cladding diameter of 22.3 μm and jacket diameter of 60.2 μm is obtained. Rotation at a rate that gives a spin-pitch of 45mm causes the holey-cladding diameter to initially increase by 23%, from 10mm at the beginning of the draw to 12.2mm at $z = L/20$ as shown in Fig. 4. Such a rate of increase is unlikely to allow the survival of the microstructured region of the fibre.

It is therefore clear that to obtain fibres with a sub-1mm spin pitch one must split the manufacture into two stages, as is often already the case [18]. The second stage of manufacture, where the preform is rotated, may then have an initial geometry much smaller than in the one-stage process. This smaller geometry allows a lower draw speed to obtain the final geometry, which in turn allows lower rotation rates for any given spin-pitch. The combined effect is to reduce significantly the geometric effects of preform rotation allowing the draw to be performed at higher temperatures. This increases the strength of the final product and allows the temperature to be varied to influence the final OD/ID ratio.

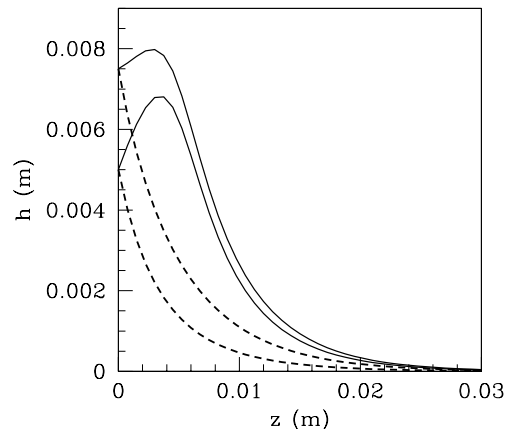


Fig. 4. The destructive effects of preform rotation on the microstructure of type-two fibres. Dashed lines show hole cladding and jacket radii of preform without rotation and solid lines show the radii with rotation.

As an example of the effects of preform rotation in such a situation consider a second-stage preform with a jacket diameter of 7mm and holey cladding 1.5mm in diameter. Without rotation, a glass temperature of 1940C, a draw speed of 1m/min and a feed speed of 1.7mm/min, the final fibre has a holey cladding of $8.6\mu\text{m}$ and a jacket diameter of $282.0\mu\text{m}$; outside the desired range described earlier. When preform rotation of 2000rpm is included to give a spin pitch of 0.5mm, these final fibre-dimensions increase to $22.8\mu\text{m}$ holey-cladding diameter and $282.8\mu\text{m}$ jacket diameter. The final OD/ID ratio, 65.4 in the absence of rotation, is decreased to 24.8. The rotation causes no initial increase in fibre dimensions towards the top of the furnace (unlike that shown in Fig. 4), suggesting that the microstructure will remain intact.

Even with the smaller initial geometry, rotation rates can be increased to the point where the holey cladding suffers a initial increase in diameter at the top of the furnace, damaging the microstructure. If the above preform is spun at 3333rpm, corresponding to a slightly smaller spin-pitch of 0.3mm, the holey-cladding diameter increases by 20% from 1.5mm at the beginning of the draw to 1.8mm at $z = L/20$. This large initial expansion of the holey cladding would surely heavily modify the microstructure. This shows the sensitivity of the holey cladding to spin rates at high temperatures and demonstrates that one must be careful to only apply the rotation necessary to achieve the final spin-pitch, having already minimized the draw speed; even with such small initial dimensions.

A two-stage drawing process allows a freedom in the initial geometry for the second stage. This should be used to choose a feed speed and initial OD/ID ratio that give the desired final OD/ID ratio.

To address the questions posed in the introduction, we first observe that the presence of a hole causes the effects of rotation on the geometry to be seen at much lower spin-rates than for solid fibres. We cannot remove fibre birefringence whilst preserving the microstructure unless a two-stage process is employed, in which case the initial geometry draw speed must be carefully chosen to prevent destruction of the microstructure. This approach has the benefit of giving an extra degree of freedom in the temperature. Preform rotation can be used to control the fibre geometry within the limits imposed by the required preservation of the microstructure as it

passes through the furnace.

4. Conclusions

An asymptotic model has been constructed and solved numerically to determine the effects on the fibre dimensions of preform rotation, to allow the reduction or removal of fibre birefringence. It was discovered that a sub-mm spin pitch could be achieved for both fibre-types considered. However, the manufacture of type-one fibres must be broken into two stages and fibre rotation may not be used as a method to control the resulting fibre geometry. For type-two fibres, care must be taken to preserve the microstructured region of the fibre, having broken the manufacture into two stages and used the second stage to prescribe the fibre geometry. The two-stage process also allows fibres to be drawn at higher temperatures, producing fibres of superior strength.

For more detail and a complete derivation of the mathematical model for the rotation of capillary tubes that forms the basis for this paper, see [13] and [19].

Acknowledgments

Tanya Monro acknowledges the support of a Royal Society University Research Fellowship. Christopher Voyce would like to thank Dr. Mark A. Brummell and Mr John R. Hayes for useful discussions.